Nuclear Physics **A422** (1984) 635–653

K^+ PRODUCTION IN A CASCADE MODEL FOR HIGH-ENERGY NUCLEUS–NUCLEUS COLLISIONS

J. CUGNON

University of Liège, Institute of Physics B5, Sart Tilman, B-4000 Liège 1, Belgium

and

R.M. LOMBARD

CEN Saclay, DPhN/ME, F-91191 Gif-sur-Yvette Cédex, France

and

SLAC, PO Box 4349, Stanford, California 94305, USA

Received 12 December 1983

Abstract: The K^+ production is studied for the p+NaF, Ne+NaF, Ne+Pb systems at 2.1 GeV/A in the frame of a 3-dimensional cascade model. Owing to the small elementary production cross sections, the K^+ production is calculated perturbatively. Two kinds of production processes are introduced: baryon–baryon collisions leading to three-particle final states, and pion–nucleon collisions leading to two-body final states. The time evolution of the two processes is studied. The integrated K^+ cross sections are in good agreement with the experimental data. The contribution of the πN induced mechanism is of the order of 25% for Ne+NaF, but increases with the size of the system. Scaling properties are discussed. A simple rescattering model is used to calculate the invariant cross section for the Ne+NaF case. Good agreement with experiment is obtained, except at forward angles.

1. Introduction

The production of positive kaons is of current interest. It has recently been suggested [1]) that the K^+'s could be formed during a stage of the collision process, where the system is compressed and highly excited. Their relatively long mean free path, compared to protons and pions would allow them to escape rather easily from the system, after some possible elastic rescattering. Indeed, it is very striking that the K^+ spectrum in the c.m. system is quite broad, indicating a "temperature" larger than the proton temperature, which in turn is larger than the pion temperature. According to ref. [1]), this suggests that the K^+'s are emitted first, and that the protons and the pions are emitted in later stages, when the system has expanded and cooled down.

The kaons present also some interest from another point of view. According to refs. [2,3]), their multiplicity, or more exactly the ratio of the multiplicities for various strange particles, could provide a signal for the formation of a quark-gluon plasma.

So far, only one experiment [4,5]), but involving several systems, has been devoted to the K^+ cross section. Yet, it covers a limited range of momentum, such that the K^+ "temperature" mentioned above does not have the same meaning as the same quantity for protons and pions, which is usually taken as the slope parameter of the 90° c.m. spectrum in a symmetric system. On the other hand, numerous calculations have been done, which fall into two main categories. We make a rapid review.

(*i*) *Thermal models.* The K^+ production has been calculated in a pure thermal and chemical equilibrium model [6]). This calculation has been refined in a so-called phase-space approach [7]). Recently [8]), a hadrochemical calculation has been carried out, where the hypothesis of chemical equilibrium is relaxed, and where the K^+'s are created (and possibly destroyed) by nuclear collisions during the expansion phase. In refs. [6,7]), the K^+ yield is greatly overestimated, whereas it comes out right in ref. [8]). Let us mention that these models contain at least one free parameter, which is related to the freeze-out density, when the fireball breaks into pieces.

(*ii*) *Multiple scattering models.* In the spirit of these models, the K^+'s are produced by the first sufficiently energetic nucleon-nucleon collisions, when the nucleon flow is still strongly aligned with the beam direction. The much more isotropic K^+ emission then arises from the almost isotropic elementary cross section and possibly from the subsequent rescattering of the K^+'s. The first calculation along these lines has been carried out by Randrup and Ko [9]), using the so-called rows-on-rows model for generating the sequence of baryon–baryon collisions. They essentially underestimated the total yield by a factor 2. The latter has since been recognized as coming from an erroneous normalization of the adopted elementary K^+ production cross sections [10,11]). The calculated c.m. distributions (for the Ne+NaF system) was much narrower than the observed one, a feature coming from the proximity of the K^+ threshold. When a reasonable rescattering [12]) of the K^+'s by the baryons is introduced, a satisfactory agreement with experiment is obtained. In ref. [13]), however, it is suggested that the rescattering by the pions is also an efficient agent of spectral broadening. Recently, the results by Randrup and Ko concerning the primordial K^+ cross sections in the Ne+NaF system has been confirmed by an intranuclear cascade model [10]) and by a diffusion model [14]).

The positive kaons can be created in two kinds of elementary collisions: either in $NN \rightarrow N\Lambda K$ and similar collisions (see below) or in $\pi N \rightarrow \Lambda K$ (and similar) collisions. The first process only is introduced in refs. [9,10,14]). The importance of the second process has been suggested by Halemane and Mekjian [15]). It has been neglected so far, except in ref. [8]), where, however, nucleons and pions are assumed to be in thermal equilibrium all the time.

This situation called, in our opinion, for a detailed calculation of K^+ production, at least for the primordial kaons, using a microscopic model for the collision process. That is our aim in this paper, where we use the intranuclear cascade model described in ref. [16]). The difference from our previous work [10]) is that here we use a version

of the numerical code which takes the pions into account explicitly [in contradistinction to ref. [10]), which considers frozen delta's]. This will allow us to calculate the $\pi N \to \Lambda K$, ΣK, the so-called Mekjian mechanism, in a reliable model, for the first time.

Our work is organized as follows. In sect. 2, we briefly describe the model. Sect. 3 contains a discussion of the input data. In sect. 4, we present our results, as well as a discussion of a few features of the calculation. Finally, sect. 5 contains our conclusion.

2. The model

The cascade code that we use is described in detail in refs. [16,17]). It is sufficient here to say that in such an approach, the collision process is viewed as a sequence of binary collisions (plus decays) between hadrons, proceeding as in free space. The code handles nucleons, Δ-resonances and pions explicitly, but does not distinguish between isospin states. The explicit treatment of the kaons would demand a profound modification of the code. We rather decided to take advantage of the small size of the elementary production cross section and turned to a perturbation scheme. We run the cascade code without reference to the kaons and record the whole sequence of binary collisions. For any event, we thus know the nature B and B′ of the partners in baryon–baryon collisions as well as their four-momenta p_B, $p_{B'}$. Similarly, we know the pion and nucleon momenta p_π, p_N in pion–nucleon collisions. In first approximation, the K^+ production cross section is given by

$$E_K \frac{d^3\sigma}{dp_K^3} = \sum_c \int 2\pi b\, db \int \frac{d^3p_B}{E_B}\frac{d^3p_{B'}}{E_{B'}} f(p_B,p_{B'}) \frac{1}{\sigma_{BB'}^{tot}(s)} E_K \frac{d^3\sigma_c}{dp_K^3}(p_B + p_{B'} \to p_K)$$
$$+ \sum_c \int 2\pi b\, db \int \frac{d^3p_\pi}{E_\pi}\frac{d^3p_N}{E_N} f(p_\pi,p_N) \frac{1}{\sigma_0} E_K \frac{d^3\sigma_{c'}}{dp_{K'}^3}(p_\pi + p_N \to p_K)\,. \qquad (2.1)$$

In this equation, $f(p_B, p_{B'})$ is the probability of having a collision between baryon B and baryon B′ with four-momenta p_B and $p_{B'}$ respectively. The index c refers to the possible reaction channels:

$$B + B' \to N\Lambda K,\ \Delta\Lambda K,\ N\Sigma K,\ \Delta\Sigma K\,, \qquad (2.2)$$

where B and B′ are either a nucleon or a Δ. In refs. [9,10,14]), these processes are solely considered. In the second term, c' runs over

$$\pi N \to \Lambda K,\ \Sigma K\,. \qquad (2.3)$$

The other symbols in eq. (2.1) have standard meaning, except σ_0, which calls for some remarks. In our cascade code, a pion and a nucleon interact in the Δ-resonance region only, whereas the process (2.3) occurs at much larger energies. We nevertheless recorded the close encounters of πN pairs in this energy range, provided the closest distance of approach is smaller than $(\sigma_0/\pi)^{1/2}$. Accordingly, $f(p_\pi, p_N)$ is the

probability distribution for such an encounter. The results should be more or less independent of the value of σ_0, provided it is larger than the integrated $\sigma_{c'}$ cross section. The latter is of the order of 1 mb. However, in order to improve the statistics, we have chosen $\sigma_0 = 10$ mb. We checked that the results do not change by more than a few percent when going to $\sigma_0 = 5$ mb in the Ne+NaF case.

The justification of the first term in eq. (2.1) relies on the small size of the ratio $\sigma_{BB}^{prod}/\sigma_{BB}^{tot} \approx 0.01$ between the elementary production cross section and the total baryon-baryon cross section. The second term in eq. (2.1) is justified by the small total yield (see later on).

For numerical purposes, eq. (2.1) is discretized as

$$E_K \frac{d^3\sigma}{dp_K^3} = \sum_c \sum_{b_i} 2\pi(\Delta b) b_i \frac{1}{N_{ev}} \sum_{ev} \sum_{\substack{coll \\ s>s_c}} \frac{1}{\sigma_{BB'}^{tot}} E_K \frac{d^3\sigma_c}{dp_K^3}(p_B + p_{B'} \to p_K)$$

$$+ \sum_{c'} \sum_{b_i} 2\pi(\Delta b) b_i \frac{1}{N_{ev}} \sum_{ev} \sum_{\substack{coll \\ s>s_{c'}}} \frac{1}{\sigma_0} E_K \frac{d^3\sigma_{c'}}{dp_K^3}(p_\pi + p_N \to p_K) , \qquad (2.4)$$

where there is a sum over the impact parameter (b_i), over the events generated (ev) and over the collisions with a squared c.m. energy larger than the square of the threshold energy for channel c. Typical values are $\Delta b \approx 0.5$–1 fm, N_{ev} (the number of events per impact parameter) = 250.

For the first channels c, the elementary cross sections are continuous functions of $\boldsymbol{p}_K$ (see below), whereas for the channels c' it contains a delta function, due to the two-body final state. To avoid this unpleasant feature, we have replaced the delta function in the πN c.m. by a step function with a width of 0.25 $p_{c.m.}$, where $p_{c.m.}$ is precisely the K-momentum in this system. This introduces an averaging procedure with a width of about 70 MeV/c. We have also verified that the results (for the angular distribution) are not very sensitive to the value of the width.

Eqs (2.1), (2.2) should be regarded as the expression for what one would call the primordial cross section. In other words, they neglect the rescattering. Therefore, this approach is particularly suited to the calculation of the integrated cross sections, since the K^+'s are essentially scattered elastically: their yield is completely independent of the detail of the rescattering. Later on, just to compare with experiment, we shall apply a simple rescattering correction.

3. Input data

3.1. THE BARYON–BARYON-INDUCED COLLISONS

For these collisions, i.e. for the channels c, we use exactly the same input data (and the same model and same isospin average) as Randrup and Ko [9], except that

we use the correct normalization [10,11]). The cross sections have the following form:

$$E_K \frac{d^3\sigma}{dp_K^3} = \sigma_c \frac{P_{max}}{m_K c} \frac{E_K}{4\pi p_K^2} \frac{12}{p_{max}} \left(1 - \frac{p_K}{p_{max}}\right) \left(\frac{p_K}{p_{max}}\right)^2 , \tag{3.1}$$

where p_{max} is the maximum c.m. momentum reached by the kaon for a given c.m. energy. The constant σ_c is the integrated cross section for $p_{max} = m_K c$. The numerical values are given in ref. [10]). The last two factors in (3.1) embody the angular distribution, which is isotropic in the c.m. The momentum dependence is close to but not exactly equal to a constant phase-space density distribution in the energy range under interest. Eq. (3.1) provides a reasonable fit to the existing data [see e.g. ref. [18])].

3.2. THE π-NUCLEON-INDUCED COLLISIONS

We give here some detail on the manner the existing experimental data can be used.

3.2.1. Isospin average. With data existing for some channels only, it is of interest to consider the isospin average. We have particularly the Ne+NaF system in mind, where this average is sufficient.

The ΛK final state being a $T = \frac{1}{2}$ state only, we obviously have

$$\sigma(\pi^0 p \to \Lambda K^+) = \tfrac{1}{3}\sigma(1) , \qquad \sigma(\pi^+ n \to \Lambda K^+) = \tfrac{2}{3}\sigma(1) , \tag{3.2}$$

where $\sigma(1)$ is the $T = \frac{1}{2}$ cross section leading to a ΛK state. In a symmetric system ($N = Z$, $N_{\pi^+} = N_{\pi^0} = N_{\pi^-}$), we have, for the average over the initial isospin states,

$$\bar{\sigma}(\pi N \to \Lambda K^+) = \tfrac{1}{4}\sigma(\pi^+ n \to \Lambda K^+) , \tag{3.3}$$

or, because of isospin symmetry,

$$\bar{\sigma}(\pi N \to \Lambda K^+) = \tfrac{1}{4}\sigma(\pi^- p \to \Lambda K^0) , \tag{3.4}$$

the latter cross section being known experimentally.

For the $\pi N \to \Sigma K$ reaction, the situation is more delicate, since we may have isospin mixing in both the final and the initial state. Here we have (for $m = +1, 0, -1$)

$$\begin{aligned} \bar{\sigma}(\pi N \to \Sigma^m K^+) = {} & \tfrac{1}{6} \sum_{m_1, m_2} \sum_{T=1/2,3/2} (1 m_1 \tfrac{1}{2} m_2 | T m + \tfrac{1}{2})^2 \sigma(2T) (1 m \tfrac{1}{2} \tfrac{1}{2} | T m + \tfrac{1}{2})^2 \\ & + \tfrac{2}{6} \sum_{m_1, m_2} (1 m_1 \tfrac{1}{2} m_2 | \tfrac{1}{2} m + \tfrac{1}{2}) (1 m_1 \tfrac{1}{2} m_2 | \tfrac{3}{2} m + \tfrac{1}{2}) \\ & \times (1 m \tfrac{1}{2} \tfrac{1}{2} | \tfrac{1}{2} m + \tfrac{1}{2}) (1 m \tfrac{1}{2} \tfrac{1}{2} | \tfrac{3}{2} m + \tfrac{1}{2}) \operatorname{Re} (\mathcal{T}_1^* \mathcal{T}_3) . \end{aligned} \tag{3.5}$$

The quantities $\sigma(1)$, $\sigma(3)$ are the cross sections for the corresponding isospin states. The last term in eq. (3.5) contains the interference between the $T = \frac{1}{2}$ and $T = \frac{3}{2}$ amplitudes. It vanishes because of the orthogonality property of the Clebsch-Gordan

coefficients. Eq. (3.5) reduces to

$$\bar{\sigma}(\pi N \to \Sigma^m K^+) = \tfrac{1}{6} \sum_T \sigma(2T)(1 m \tfrac{1}{2}\tfrac{1}{2} | T m + \tfrac{1}{2})^2 , \tag{3.6}$$

or

$$\bar{\sigma}(\pi N \to K^+ + \text{any } \Sigma) = \tfrac{1}{6}(\sigma(1) + 2\sigma(3)) . \tag{3.7}$$

The latter quantity may be related to experimentally known cross sections, *provided the interference terms are neglected* when considering a particular channel. We shall adopt this procedure here without having any justification for it. It is then easy to show that

$$\bar{\sigma}(\pi N \to K^+ + \text{any } \Sigma) = \tfrac{1}{4}\{\sigma(\pi^- p \to \Sigma^- K^+) + \sigma(\pi^- p \to \Sigma^0 K^0) + \sigma(\pi^+ p \to \Sigma^+ K^+)\} . \tag{3.8}$$

3.2.2. Integrated cross sections. The experimental cross sections entering in eqs. (3.4) and (3.8) are known with reasonable precision. They are given in fig. 1 ($\pi^- p \to \Lambda K^0$), fig. 2 ($\pi^+ p \to \Sigma^+ K^+$) and fig. 3 ($\pi^- p \to \Sigma^- K^+$ and $\pi^- p \to \Sigma^0 K^0$). In the same figures are given simple approximations to describe the data. They can be written as

$$\sigma(\pi^- p \to \Lambda K) = 0.9 \text{ mb} \frac{\sqrt{s} - \sqrt{s_0}}{0.091 \text{ GeV}} , \tag{3.9a}$$

for $\sqrt{s_0} = m_\Lambda + m_K < \sqrt{s} < 1.7$ GeV,

$$\sigma(\pi^- p \to \Lambda K) = \frac{90 \text{ MeV·mb}}{\sqrt{s} - 1.6 \text{ GeV}} , \tag{3.9b}$$

for $\sqrt{s} > 1.7$ GeV,

$$\sigma(\pi^+ p \to \Sigma^+ K^+) = 0.7 \text{ mb} \frac{\sqrt{s} - \sqrt{s_0}}{0.218 \text{ GeV}} , \tag{3.10a}$$

for $\sqrt{s_0} = m_{K^+} + m_{\Sigma^+} < \sqrt{s} < 1.9$ GeV,

$$\sigma(\pi^+ p \to \Sigma^+ K^+) = \frac{140 \text{ MeV·mb}}{\sqrt{s} - 1.7 \text{ GeV}} , \tag{3.10b}$$

for $\sqrt{s} > 1.9$ GeV, and

$$\tfrac{1}{2}[\sigma(\pi^- p \to \Sigma^- K^+) + \sigma(\pi^- p \to \Sigma^0 K^0)] = 0.25 \text{ mb} \times [1 - 0.75 \text{ GeV}^{-1} \times (\sqrt{s} - 1.682 \text{ GeV})] , \tag{3.11}$$

for $\sqrt{s} > 1.682$ GeV, which is the average threshold. As fig. 3 indicates, the latter approximation is poorer than (3.9) and (3.10), because of the large dispersion of the experimental points. Furthermore, it slightly overestimates the data between 2.2 and 2.6 GeV, but this has no significant consequences, as we shall see later.

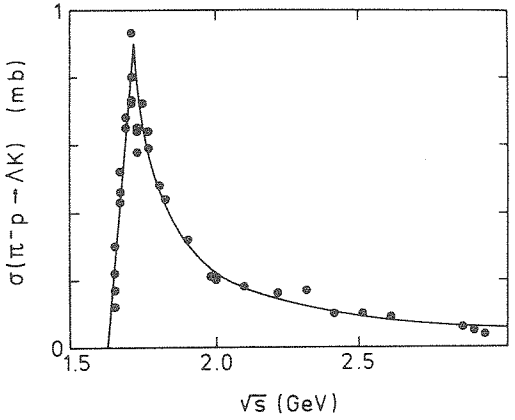

Fig. 1. Experimental (dots) $\pi^- p \to \Lambda^0 K^0$ cross section, taken from ref. [19]). The uncertainties are typically of 5 to 10%. The quantity $\sqrt{s}$ is the c.m. energy. The full curve gives a simple parametrization (see text).

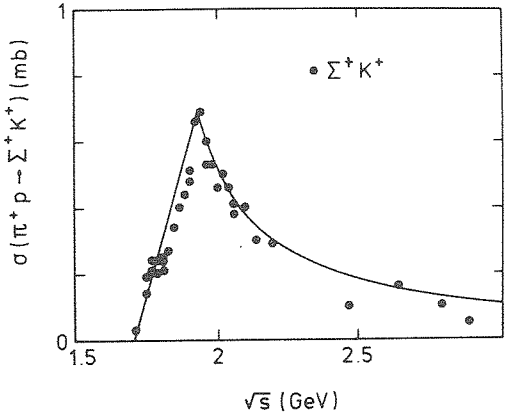

Fig. 2. Same as fig. 1, for $\pi^+ p \to \Sigma^+ K^+$.

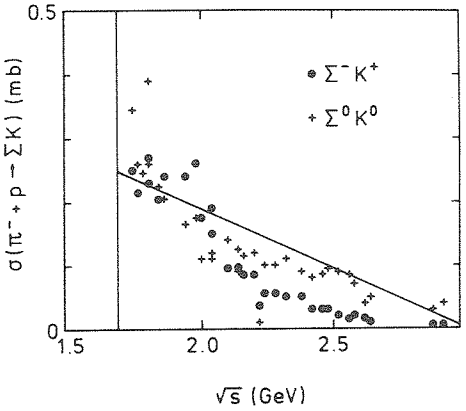

Fig. 3. Experimental $\pi^- p \to \Sigma^- K^+$ and $\pi^- p \to \Sigma^0 K^0$ cross sections, taken from ref. [19]). Typical uncertainties are of the order of 10% for both channels. The full line gives a simple parametrization for the cross section averaged over the two channels.

3.2.3. Differential cross sections. The experimental information concerning the angular distribution of the outgoing kaons in the πN-induced reactions is very sparse and fragmentary. Moreover, the distribution shows a very rich structure sometimes changing rapidly with energy in the domain under interest. We preferred to keep the calculation at the lowest level of complexity and looked at the simplest way of characterizing the angular distribution. Fortunately, as we shall see, the results are not very sensitive to this part of the input data.

The simplest quantity one may think of is the forward–backward asymmetry. If the K^+ angular distribution in the c.m. system is expanded in Legendre polynomials,

$$f(\theta) = 1 + \sum_{l=1} A_l P_l(\cos\theta)\,, \tag{3.12}$$

the forward–backward ratio is given by

$$\frac{F}{B} = \frac{1 + \sum_{l\geq 1} A_l \int_0^1 P_l(x)\,\mathrm{d}x}{1 + \sum_{l\geq 1} A_l \int_{-1}^0 P_l(x)\,\mathrm{d}x}\,. \tag{3.13}$$

This gross information is also carried by the quantity A_1^{eff}, that is defined as the coefficient of a distribution $f^*(\theta)$ involving only Legendre polynomials up to first order,

$$f^*(\theta) = 1 + A_1^{\mathrm{eff}} \cos\theta\,, \tag{3.14}$$

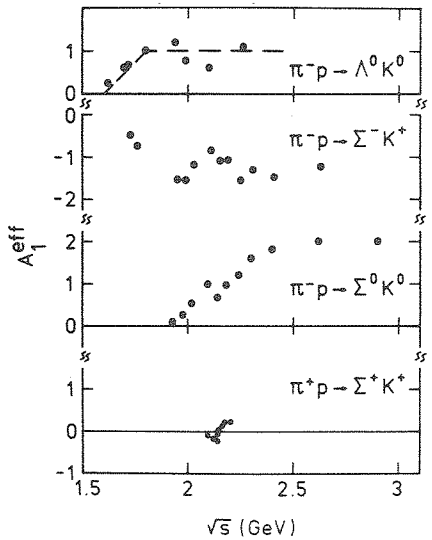

Fig. 4. Quantity A_1^{eff} (see text) as a function of the c.m. energy $\sqrt{s}$, for various experimentally investigated channels. Data from refs. [21–23]) are used.

which yields the same F/B ratio as (3.13). Of course, one has

$$A_1^{\text{eff}} = 2 \sum_{l \geq 1} A_l \int_0^1 P_l(x)\, dx. \tag{3.15}$$

The coefficient A_1^{eff} is given in fig. 4 for the previously mentioned channels. For the $\pi N \to \Lambda K$ channel, we adopted the distribution (3.14), with a simple parametrization of the energy dependence of A_1^{eff} as given by the long dashes in fig. 4.

A somewhat different procedure is chosen for the $\pi N \to \Sigma K$ channels. Since we use isospin average only, we would wash out the clear backward emission in the $\pi^- p \to \Sigma^- K^+$ reaction and the clear forward emission in $\pi^- p \to \Sigma^0 K^0$. Therefore, we chose the following distribution for the $\pi N \to \Sigma K$ channels:

$$\tilde{f}(\theta) = 1 + A_1^{\text{eff}} |\cos\theta| \tag{3.16}$$

with $A_1^{\text{eff}} = 1$, independent of the energy.

4. Results

4.1. THE Ne+NaF SYSTEM

4.1.1. Time evolution. The number of binary collisions per unit time is given as a function of time in fig. 5, for central ($b = 0$) collisions, along with the baryon density at the c.m. of the system. As expected, the baryon–baryon collisions able to produce a kaon are frequent at the beginning of the collision process, when the

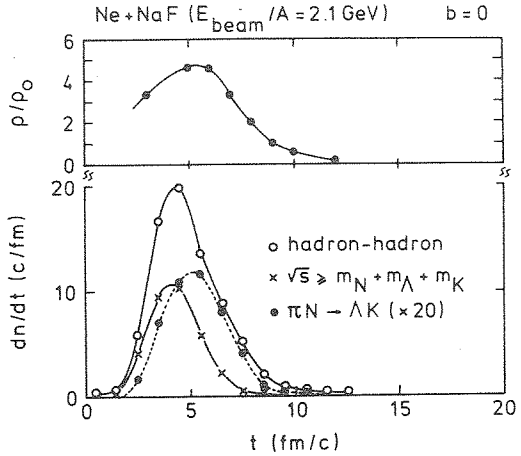

Fig. 5. The upper part gives the time evolution of the baryon density at the c.m. of the system in central ($b = 0$) Ne+NaF collisions. The latter is evaluated by counting the particles in a sphere of radius equal to 1 fm. The lower part of the figure gives the number of collisions per unit time: hadron–hadron collisions (open dots), baryon–baryon collisions with an energy above the NΛK threshold (crosses), and pion–nucleon collisions with an energy above the ΛK threshold.

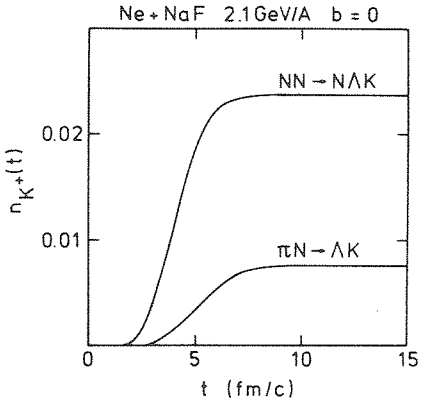

Fig. 6. Time evolution of the K^+ multiplicity, coming from two particular reactions in central Ne+NaF collisions.

system is compressed. The πN collisions that can generate a kaon take place later, because of the time span required to create pions. Due to the spatial extension of the system, the time separation between the two generations of kaons is not as clean as one would guess at first sight.

Fig. 6 shows the time evolution of the K^+ population for the two generations. If dn/dt denotes the rate of baryon–baryon collisions above the NΛK threshold (crosses in fig. 4), one may write for the first generation

$$\frac{dn_{K^+}}{dt} \propto \frac{dn}{dt} \langle \sigma v \rangle , \tag{4.1}$$

where $\langle \sigma v \rangle$ means an average over the relative velocity. Close examination of figs. 4 and 5 shows that dn/dt is the crucial factor for the evolution of K^+ population, although $\langle \sigma v \rangle$ steadily decreases as time proceeds. The same remark applies to the second generation, with still a slower variation of $\langle \sigma v \rangle$.

4.1.2. Energy distribution versus cross sections. Figs 7 and 8 give an idea of the interplay between the πN cross sections and the distribution of the c.m. energy for the πN pairs (integrated over the whole duration of the Ne+NaF collision). The latter is given by the histograms. As expected, this function is rapidly decreasing in this energy range. The maximum of this distribution would be around 1.2 GeV and therefore only the tail of this distribution plays a role. The net effect of this distribution weighted by the production cross section is illustrated by the open dots in figs. 7 and 8. One may realize from fig. 7 that, in view of the rapid variation of the cross section, an estimate of the K^+ yield in the second generation should be based on a reliable model, like ours, for the πN energy distribution. This is particularly true for the $\pi N \rightarrow \Lambda K$ process, and for the $\pi^+ p \rightarrow \Sigma^+ K^+$ process, but the situation is less crucial for the $\pi^- p$ reactions. Fig. 7 also shows that πN reactions creating a K^+ in three-body final states (like $\Lambda K \pi$), that are neglected in our

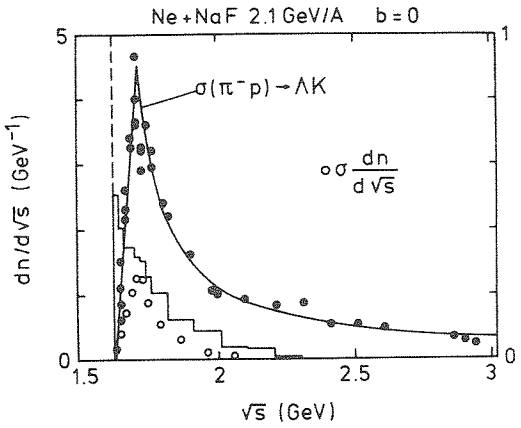

Fig. 7. Central ($b = 0$) Ne+NaF collisions. The $\pi^- p \to \Lambda K$ cross section is given in mb by the scale on the right. The histogram displays the distribution $dn/d\sqrt{s}$ of the πN collisions (for the whole collision process), according to their c.m. energy $\sqrt{s}$. It is only given for $\sqrt{s}$ larger than the ΛK threshold. The scale is on the left. The open dots give the product of the $\pi^- p \to \Lambda K$ cross section by the function $dn/d\sqrt{s}$ (in arbitrary units).

calculation, would play a minor role. Indeed, the latter reactions channels open around 1.9 GeV and the corresponding cross sections culminate at ~0.2 mb around 2.1 GeV [ref. [19]].

4.1.3. Sensitivity upon the angular distribution of the πN reactions. We have investigated this sensitivity by making a calculation with an isotropic distribution and compared with a calculation using eqs. (3.14) and (3.16). The results are

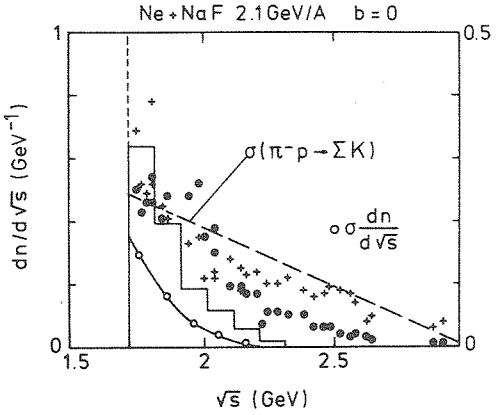

Fig. 8. Same as fig. 7, for the $\pi^- p \to \Sigma K$ cross section (see also fig. 3).

displayed in fig. 9 for the contribution of the $\pi N \to \Lambda K$ channnel alone. One may conclude a large insensitivity except at 80°. The $\pi N \to \Sigma K$ contribution (not shown) is even (significantly) more independent of the detail of the angular distribu-

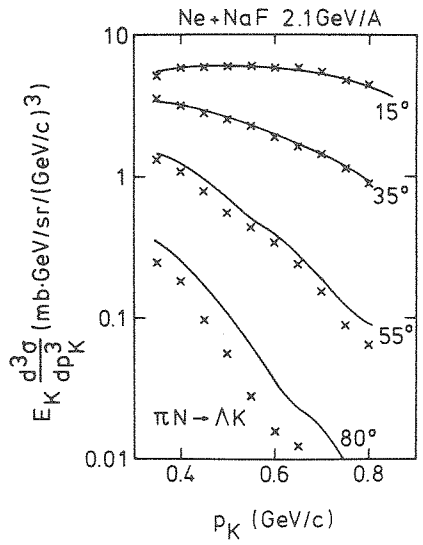

Fig. 9. Contribution of the $\pi N \to \Lambda K$ process to the invariant K^+ production cross section. The crosses correspond to a K^+ angular distribution given by eq. (3.14) (with values taken from fig. 4) in the elementary $\pi N \to \Lambda K$ reaction. The full curve is obtained when an isotropic distribution is adopted.

tion. These observations force one to admit that the πN pairs are fairly randomized in momentum space, though not completely. That is why the 80° spectrum changes with the angular distribution of the elementary processes.

4.1.4. K^+ cross sections. We do not present here the pion and proton cross sections. We have, of course, calculated these quantities. The quality of the agreement is as good as the one of our previous calculation [10]), and confirms, once more, that the intranuclear cascade model provides a satisfactory picture of the collision mechanism in the 1–2 GeV energy range.

The integrated K^+ production cross section is given in table 1 as well as its splitting over the various channels. The baryon–baryon induced reactions contribute to a cross section of 19.87 mb. The so-called Mekjian mechanism (πN reactions) increases this amount by ~25%, bringing the calculated total cross section in agreement with the experimental value. In table 1, we quote, for the sake of comparison, the results [see ref. [10])] with the version of our cascade code, which keeps the Δ's frozen during all the reaction time. There is practically no difference between the two versions as far as the baryon–baryon contribution is concerned.

We have emphasized that our calculation is primarily devoted to the calculation of the integrated cross section. Nevertheless, we attempt in figs. 10 and 11 a comparison with the experimental differential cross sections. For this reason, we apply to our primordial K^+ cross section a rescattering correction, as already described in ref. [10]). Essentially, this correction is the one which should apply if the K^+ were rescattered once by the nucleons acting as a thermal bath [20]). We assume

TABLE 1

Integrated cross sections (mb)

System	Model	BB→NΛK	BB→NΣK	BB→ΔΣK	BB→ΔΣK	Sum BB→
Ne+NaF	with π's	9.26	6.97	2.29	1.35	19.87
	no π	9.24	6.94	2.18	1.28	19.66
p+NaF	with π's	0.778	0.581	0.134	0.048	1.541
		0.584	0.363	0.100	0.030	1.077
Ne+Pb	with π's	169.48	112.34	45.93	28.24	356
		52.03	45.27	14.10	11.49	122.89

System	Model	πN→ΛK	πN→ΣK	Sum πN→	Total	Exp [refs. [4,5])]
Ne+NaF	with π's	2.83	2.90	5.73	25.60	23±8
	no π	—	—	—	—	
p+NaF	with π's	0.120	0.101	0.221	1.762	
		0.060	0.051	0.111	1.188	1.8±0.6
Ne+Pb	with π's	101.7	113.8	215.5	571.3	
		50.87	56.88	107.75	230.6	250±90

For the Ne+NaF system, the first line corresponds to the present calculation and the second line describes the results of ref. [10]), which uses a cascade model with frozen delta's. Both for p+NaF and Ne+Pb, the first line gives the cumulated ($K^+ + K^0$) cross section. The second line corresponds to the K^+ cross section (see text for details).

that the latter has a temperature of 125 MeV, consistent with the slope parameter of the proton 90° c.m. spectrum. The frequency of the rescattering is dictated by geometrical considerations [see ref. [10])]. The K^+'s of the second generation appearing later, they are probably rescattered less frequently. Therefore, we present the results without (fig. 10) and with (fig. 11) rescattering for the second-generation kaons. The agreement becomes better without rescattering, but no definite conclusion can be drawn, except that the difference between the calculated primordial spectra (dot-and-dashed curve in fig. 11) and the experimental data is likely describable by rescattering. The 15° invariant cross section is however overestimated†, which might indicate a non-isotropic rescattering, contrary to our simple picture of heat bath.

4.2. THE p+NaF AND Ne+Pb SYSTEMS

Our cascade code assumes an isospin degeneracy. Therefore, we have to apply a correction to our results in order to account for this feature. We may write for the

† This seems to be a systematic feature of the existing calculations. See refs. [9,10,14]).

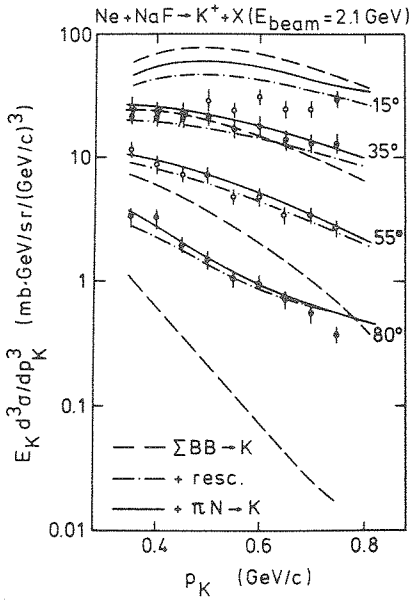

Fig. 10. Calculated invariant K^+ production cross section for several angles, compared to the data of ref. [4]). The long dashes give the contribution to the primordial cross section coming from the baryon–baryon collisions. The dash-and-dot curve is obtained by applying a rescattering correction to the first quantity (see text, for more detail). The full curve is finally obtained after addition of the πN contributions (without rescattering correction).

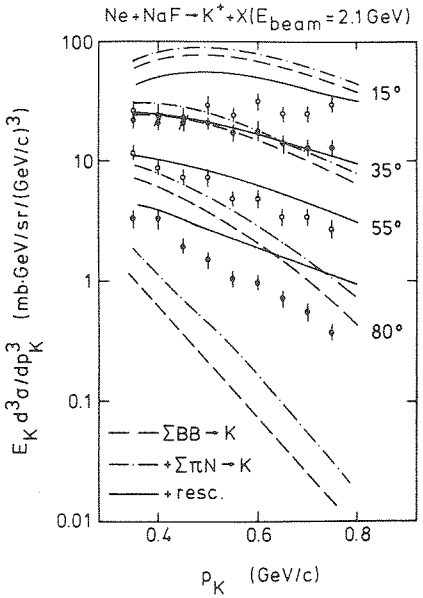

Fig. 11. Same as fig. 10, except that a rescattering correction is applied to both contributions (see text).

nucleon–nucleon-induced reactions

$$\frac{N(K^+)}{N(K^+)+N(K^0)}=\frac{xN_{pp}+\frac{1}{2}N_{pn}+(1-x)N_{nn}}{N_{pp}+N_{pn}+N_{nn}}, \tag{4.2}$$

where x is the branching ratio relevant to the final states containing a K^+, and where N_{pp} is the number of proton–proton collisions. We shall assume that the Δ's do not change this ratio significantly. For the first-generation kaons created in the p+NaF reaction, one may consider that they are created by the very first collisions ($N_{pp}=N_{pn}$, $N_{nn}=0$).

Taking the branching ratios of ref. [9]), one finds

$$\frac{N(K^+)}{N(K^+)+N(K^0)}\approx\tfrac{3}{4}\text{ and }\tfrac{5}{8}, \tag{4.3}$$

for the $X\Lambda K$ and $X\Sigma K$ channels, respectively. It is reasonable to consider that the second-generation kaons are produced in a more or less symmetric system and to adopt a ratio of $\frac{1}{2}$ for this case. Anyway, in table 1, we report on the $(K^+ + K^0)$ cross section (first line) and on the K^+ cross section obtained by using the above-mentioned branching ratios (second line). The estimated $p+NaF\rightarrow K^+ + X$ cross section is somewhat too small, but one has to keep in mind that the secondary collisions would restore somehow the isospin symmetry. Therefore, the quoted value for the first-generation contribution should be considered as a lower limit.

We attempt a similar estimate for Ne+Pb, using as a rough estimate $N_{pp}:N_{pn}:N_{nn}\approx\frac{1}{2}Z^2:NZ:\frac{1}{2}N^2$, where Z and N are the proton and neutron numbers of the compound system, respectively. This is in keeping with the fact that the secondary collisions are more important in an extended system. For the kaons of the second generation, we still keep a factor $\frac{1}{2}$, because the neutron excess would in some sense be compensated by π^+ excess. With these considerations, our estimate comes in agreement with the total experimental cross section, which is, however, measured with a 35% accuracy.

For the sake of completeness, we present in figs. 12 and 13 the calculated invariant cross sections. Here, we did not attempt to apply a rescattering correction, since the latter is presumably very intricate and certainly not isotropic in the c.m. It is perhaps surprising that in the p+NaF system the situation still demands a substantial rescattering.

4.3. SCALING

The reduced cross sections, i.e. the total $K^+ + K^0$ cross sections divided by the product AB of the mass numbers of the partners, are shown in table 2. They give more insight into the nature of the two generations. For the first one, the reduced cross section is roughly constant over the three systems under consideration. This

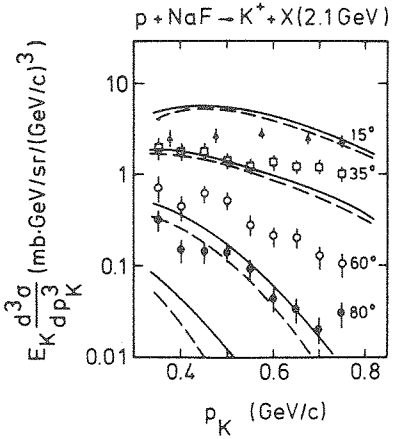

Fig. 12. Calculated invariant K^+ production cross section for p+NaF collisions, at various angles, compared to the data of ref. [5]). The dashed curve corresponds to the contribution from the baryon–baryon collisions. The full curve is obtained by adding the contribution of the πN collisions.

TABLE 2

Reduced ($K^+ + K^0$) cross sections (μb)

System	BB→XΛK	πN→XK	total
p+NaF	77 (102)	11	88
Ne+NaF	98 (90)	29	127
Ne+Pb	86 (70)	52	137

The numbers between parentheses are taken from Randrup and Ko [9]), after correction (see text). The remaining numbers are from our results.

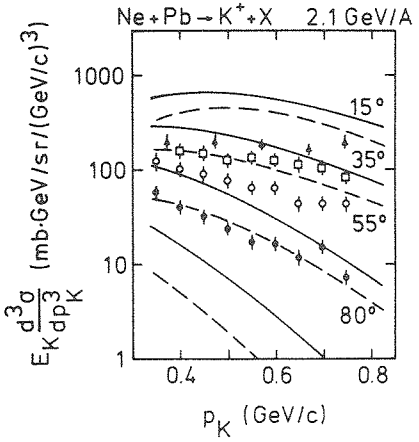

Fig. 13. Same as fig. 12, for Ne+Pb collisions.

property is very suggestive of the generations by first collisions, as already emphasized by Randrup and Ko [9]) in their original paper. On the other hand, the reduced cross section for the second generation increases with the size of the system. The latter property may be understood, according to us, as follows. One may write, as an illustrative formula,

$$N_K \propto \overline{N_\pi} N_N \langle \sigma v \rangle \Delta t , \tag{4.4}$$

where N_π is the number of pions present in the system. The latter is not constant but increases with time. That is why we consider the average. Nevertheless, N_π is an increasing function of the number of participants. It also depends upon the temperature of the system. The latter is however expected to decrease somewhat when going from Ne+NaF to the very asymmetric system Ne+Pb. Except for this rather small effect, the product $\overline{N_\pi} N_N$ is thus roughly proportional to AB for the three systems we investigate here. This is supported by fig. 14, which shows the K^+ multiplicity m_{K^+} as a function of the impact parameter; there is a rough proportionality between m_{K^+} (for both generations, in fact) and the number of participants evaluated in a clean-cut geometry. (The same pattern exists for the Ne+Pb system (not shown).)

The quantity $\langle \sigma v \rangle$ is mainly determined by the "temperature" and not by the geometrical properties of the system. Finally, the time duration Δt of the generation increases with the size of the system and is very likely responsible for the increase of the reduced cross section for the second generation. Indeed, Δt may be estimated as the width of the dashed curve in fig. 5 for the Ne+NaF system: $\Delta t \approx 5$ fm/c. A similar plot for Ne+Pb yields $\Delta t \approx 9$ fm/c, which is consistent with the variation of the reduced cross section. We underline that relation (4.4) relies on a thermal model, but describes only the creation stage of the K^+ particles. The cross section

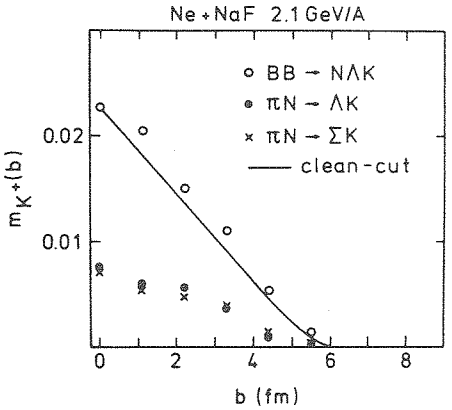

Fig. 14. K^+ multiplicity as a function of impact parameter (b) corresponding to several reactions. The full curve is the number of participant nucleons in a clean-cut geometrical picture. It is normalized to the first open dot to facilitate comparison.

σ is so small that, during the collision, the destruction process does not have any significant effect. Further, as ref. [6]) indicates, the expansion of the system cuts the chemical equilibration process very early. This is also the conclusion of ref. [8]), although they find a more important contribution of the Mekjian mechanism compared to our calculation. This may be due to a lower expansion rate in their calculation or in their assumption of thermal distribution for pions and nucleons, which may exaggerate the high-energy tail in comparison with a cascade calculation.

5. Concluding remarks

We have made an intranuclear cascade calculation of the K^+ production for three systems at 2.1 GeV per nucleon beam energy. The kaon production is introduced perturbatively, owing to the small elementary production cross sections. The emphasis should then be put on the integrated cross section, which is insensitive to final-state interactions.

We first discuss the accuracy of the evaluation of this quantity. It is directly determined by the accuracy with which the binary collisions distribution is evaluated and by the degree of knowledge of the elementary K^+-producing cross sections. As for the first quantity, we may consider that an intranuclear cascade like ours provides the best description available nowadays. Note, however, that a good description of the first very energetic collisions is also provided by the rows-on-rows model [9]), as well as by the diffusion model of ref. [14]). For the πN collisions creating kaons, our calculation provides the first detailed description of the energy distribution.

One may wonder whether the elementary cross sections are known with sufficient precision. Fig. 7 tells us that the $\pi N \to \Lambda K$ cross section is measured with a reasonable precision in the energy region where its influence is the largest (open dots in fig. 7). This is also the case for the $\pi^+ p \to \Sigma^+ K^+$ cross section, but the situation deteriorates in the $\pi^- p \to \Sigma K$ case. We recall also that our isospin-average procedure introduces some uncertainty. But altogether one may consider that for the kaons of the second generation the elementary cross sections are rather well known.

The situation is more or less reversed for the first generation. Here, one may be confident in the baryon–baryon energy distribution, which is mainly determined by the state of the system in the entrance channel. But a plot similar to fig. 7 for the $pp \to p\Lambda K^+$ cross section reveals that the collisions are the most important around $\sqrt{s} \approx 2m_p + 850$ MeV (with however a broad distribution). A look at the data [see refs. [9,10])] shows that the accuracy of our calculation of the first generation yield is then of the order of 10%, due to a corresponding uncertainty in the measurements.

Our calculation has confirmed that the kaons are generated in two very different generation processes, more or less separated in time. The first generation takes place in the early energetic nucleon–nucleon collisions, whereas the second one happens in a later stage where the motion is much more randomized. Unfortunately, the two kinds of kaons do not seem to have markedly different properties. Con-

sequently, it will be hard to distinguish experimentally between the two generations. Correlation experiments, which would be helpful in this respect, are not feasible for the moment, due to the much too low yields.

The integrated cross sections are well explained by a multiple scattering model, like our cascade model, and do not seem to require exotic processes. The uncertainties (both experimental and theoretical) do not, however, allow one to draw any definite conclusion.

The large width of the K^+ momentum distribution seems to be compatible with an ordinary production mechanism (as described here) followed by a rescattering of the kaons [see also refs. [9,10,14])]. The rescattering of the kaons by the nucleons is very efficient for broadening the K^+ distribution in momentum space, even if the K^+'s are rescattered once only, because of the smaller mass of the kaons. However, only a detailed dynamical description of the K^+ rescattering can remove the remaining ambiguities.

One of us (J.C.) is very grateful to the members of the DPhN/ME (Saclay), where part of this work was done, and for the kind hospitality extended to him during his stay. We have benefitted from a useful discussion with Dr. M.-C. Lemaire.

References

1) S. Nagamiya, Phys. Rev. Lett. **49** (1982) 1383
2) J. Rafelski and M. Danos, Phys. Lett. **97B** (1980) 279
3) J. Rafelski and B. Müller, Phys. Rev. Lett. **48** (1982) 1066
4) S. Schnetzer, M.C. Lemaire, R.M. Lombard, E. Moeller, S. Nagamiya, G. Shapiro, H. Steiner and I. Tanihata, Phys. Rev. Lett. **49** (1982) 989
5) S. Schnetzer, Ph.D. thesis, Lawrence Berkeley Laboratory
6) F. Asai, H. Sato and M. Sano, Phys. Lett. **98B** (1981) 19
7) F. Asai, Nucl. Phys. **A365** (1981) 519
8) T.S. Biró, B. Lukács, J. Zimányi and H.W. Barz, Nucl. Phys. **A386** (1982) 617
9) J. Randrup and C.M. Ko, Nucl. Phys. **A343** (1980) 519
10) J. Cugnon and R.M. Lombard, Phys. Lett. **134B** (1984) 392
11) J. Randrup and C.M. Ko, Nucl. Phys. **A411** (1983) 537
12) J. Randrup, Phys. Lett. **99B** (1981) 9
13) C.M. Ko, Phys. Rev. **C23** (1981) 2760
14) W. Zwermann, B. Schürmann, K. Dietrich and E. Martschew, Phys. Lett. **134B** (1984) 397
15) T.R. Halemane and A.Z. Mekjian, Phys. Rev. **C25** (1982) 2398
16) J. Cugnon, T. Mizutani and J. Vandermeulen, Nucl. Phys. **A352** (1981) 505
17) J. Cugnon, D. Kinet and J. Vandermeulen, Nucl. Phys. **A379** (1982) 553
18) J. Bystricky and F. Lehar, Phys. Data **11-1** (Pt. I) (1978) 110
19) Compilation of cross sections (I) π^- and π^+ induced reactions, The High-Energy Reaction Analysis Group, report CERN-HERA 79-01 (1979)
20) H.J. Pirner and B. Schürmann, Nucl. Phys. **A336** (1980) 508
21) O. Goussu *et al.*, Nuovo Cim. **62A** (1966) 606
22) O.I. Dahl *et al.*, Phys. Rev. **163** (1967) 1430
23) G.E. Kalmus, G. Borreani and L. Louie, Phys. Rev. **D2** (1970) 1824